Supporting Information

Vacancy controlled n-p conduction type transition in CuAgSe with superior thermoelectric performance

Tian Yu[a], Suiting Ning[a], Tingting Zhang[a], Xiangbin Chen[a], Qian Liu[a], Ning Qi[a], Zhiquan Chen*[a], Xianli Su[b] and Xinfeng Tang[b]

[a]Hubei Nuclear Solid Physics Key Laboratory, Department of Physics, Wuhan University, Wuhan 430072, China

[b]State Key Laboratory of Advanced Technology for Materials Synthesis and Processing, Wuhan University of Technology, Wuhan 430072, China

E-mail: chenzq@whu.edu.cn

Supplementary Figures

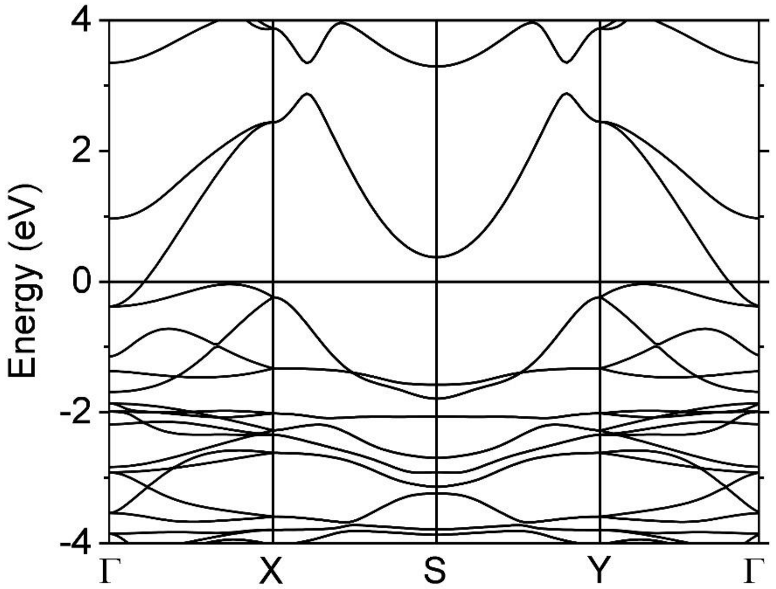

Fig. S1 The calculated band structure of β-CuAgSe.

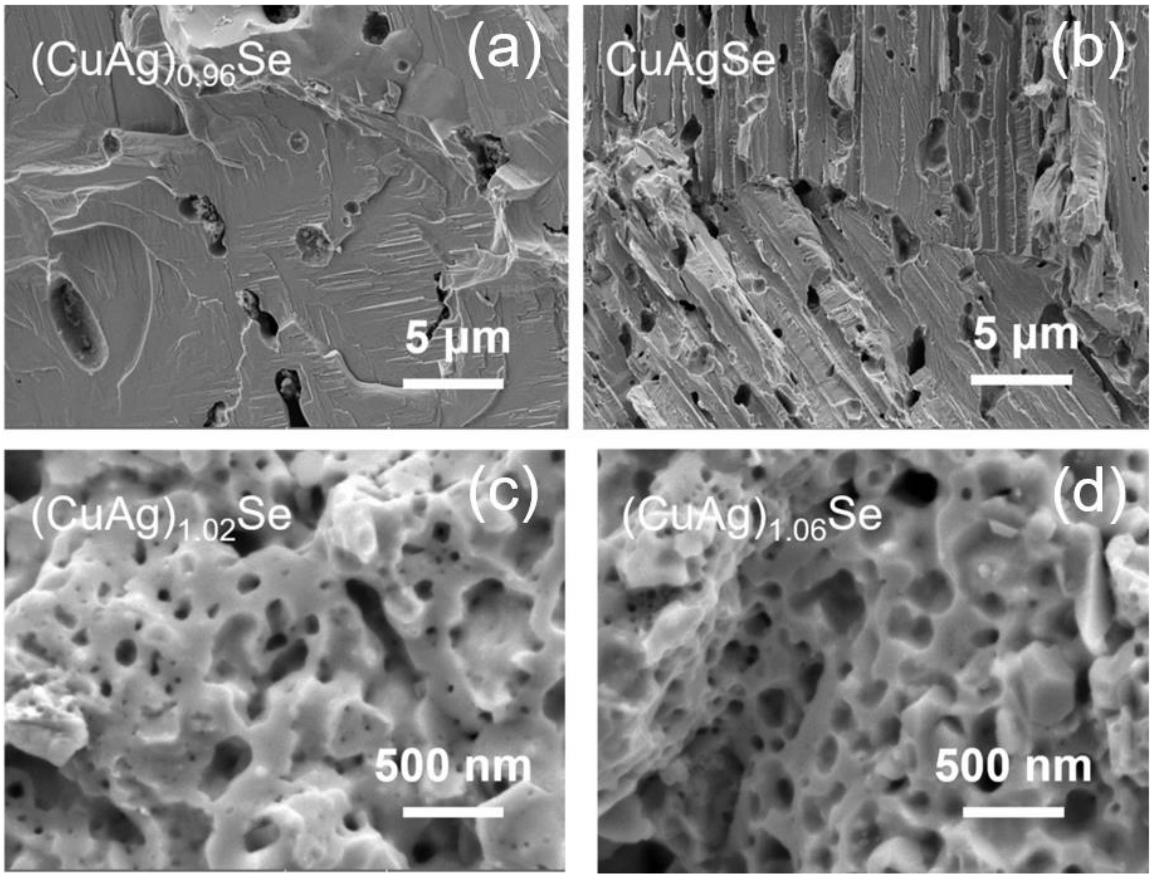

Fig. S2 SEM images of fracture morphology for (a) $(CuAg)_{0.96}Se$, (b) CuAgSe, (c) $(CuAg)_{1.02}Se$, (d) $(CuAg)_{1.06}Se$.

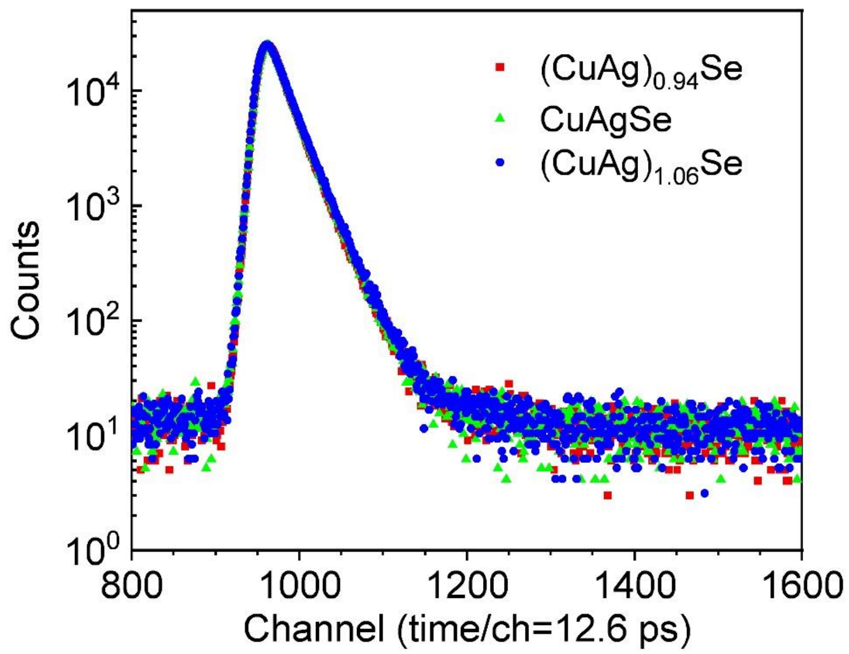

Fig. S3 Positron lifetime spectra of $(CuAg)_{0.94}Se$, CuAgSe and $(CuAg)_{1.06}Se$.

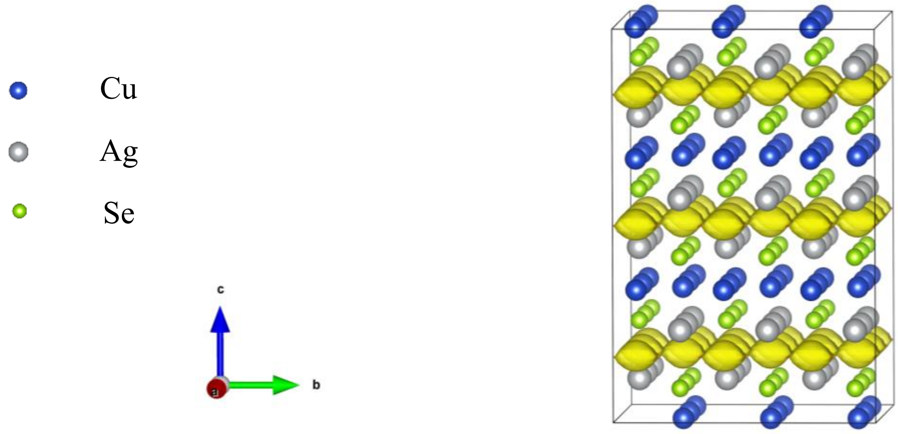

Fig. S4 Positron density distribution in the bulk state of CuAgSe.

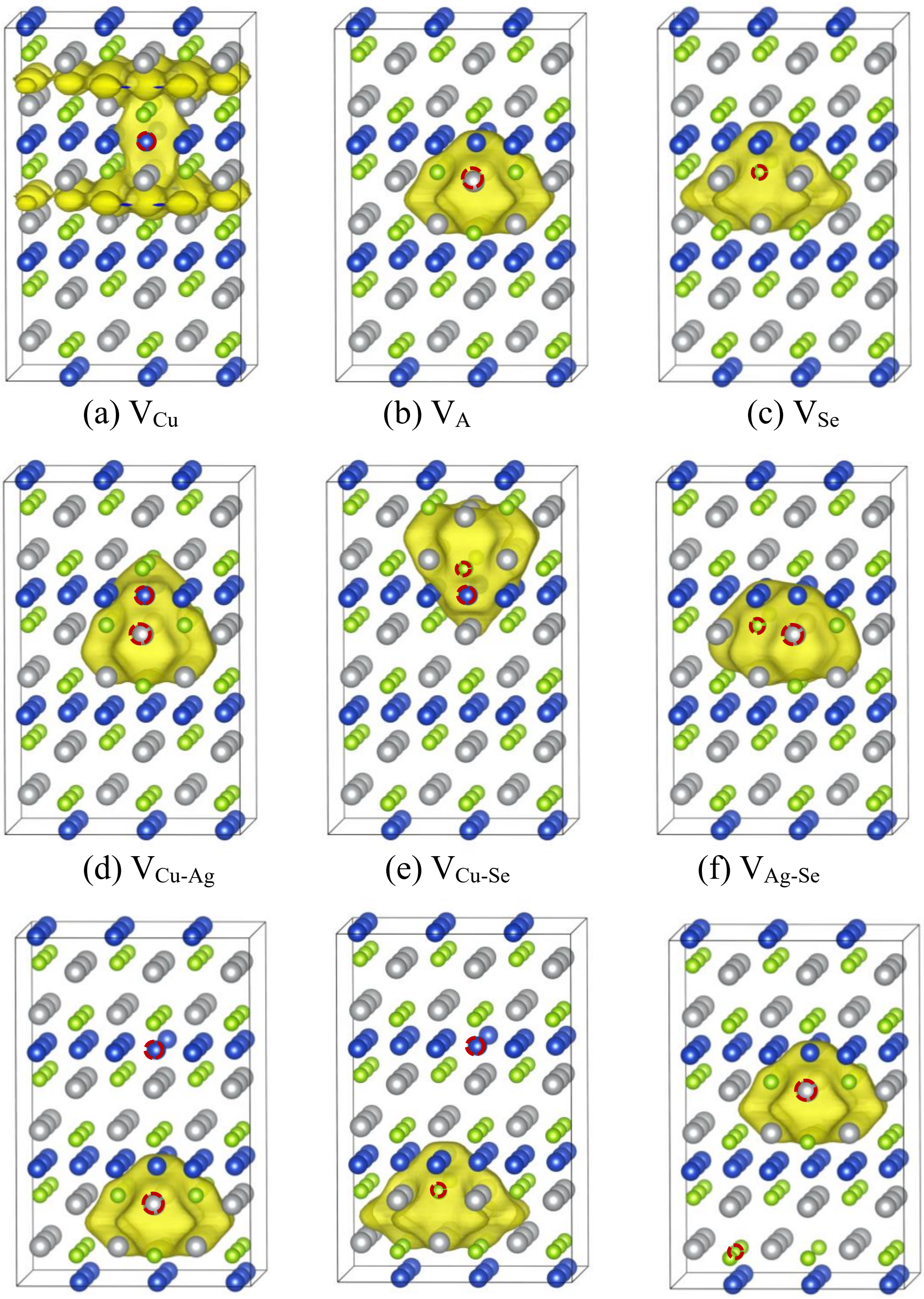

(a) V_{Cu} (b) V_{A} (c) V_{Se}

(d) $V_{Cu\text{-}Ag}$ (e) $V_{Cu\text{-}Se}$ (f) $V_{Ag\text{-}Se}$

(g) $V_{Cu}+V_{Ag}$ (h) $V_{Cu}+V_{Se}$ (i) $V_{Ag}+V_{Se}$

Fig. S5 Positron density distribution in the trapping state with various defects in CuAgSe.

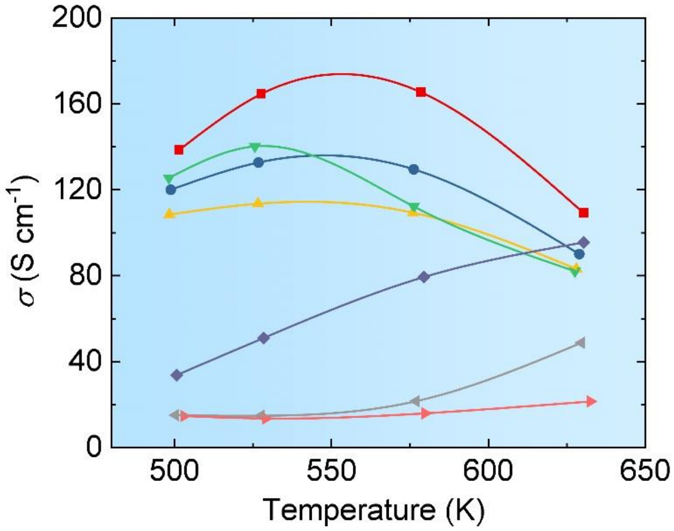

Fig. S6 Temperature-dependent conductivity of $(CuAg)_xSe$ (x = 0.94, 0.96, 0.98, 1, 1.02, 1.04, 1.06) after phase transition.

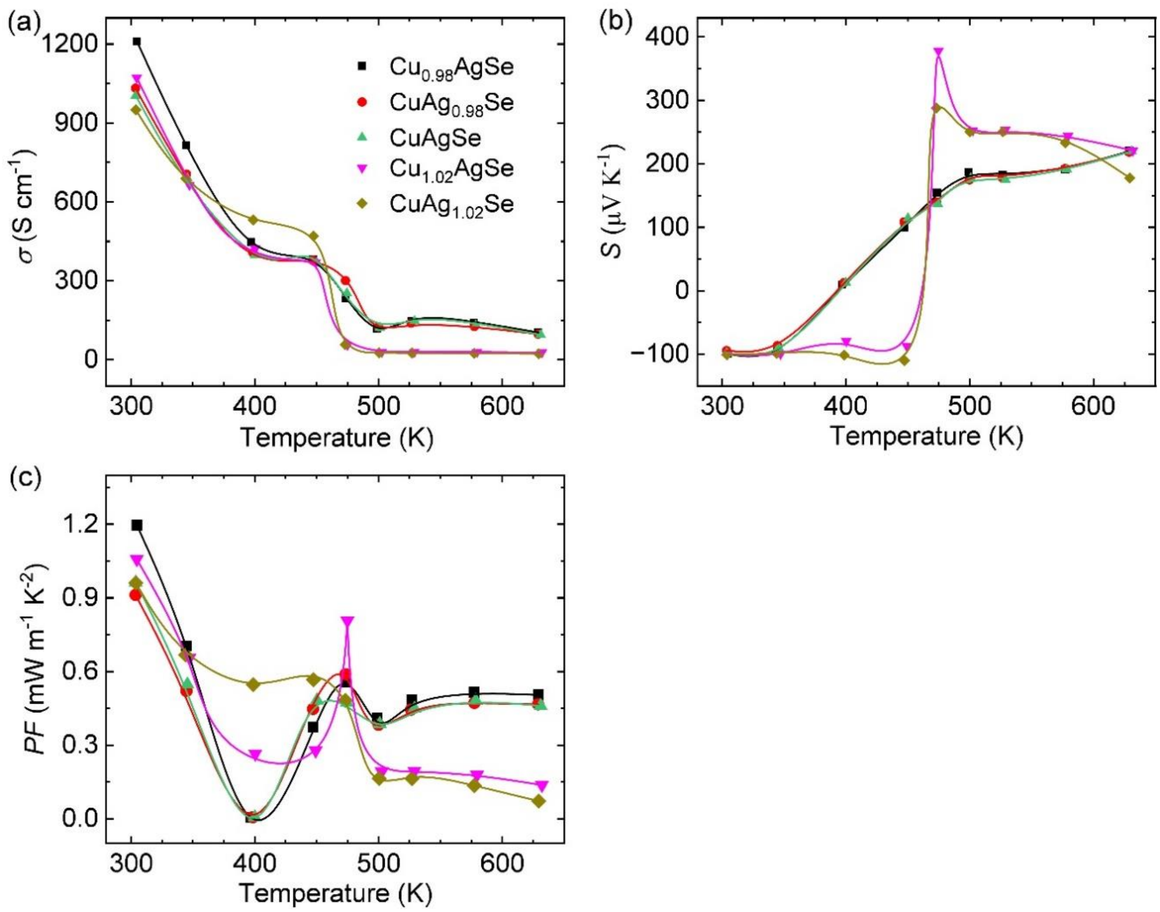

Fig. S7 The temperature-dependent electric transport properties of $Cu_{1.02}AgSe$, $CuAg_{1.02}Se$, CuAgSe, $Cu_{0.98}AgSe$, $CuAg_{0.98}Se$: (a) conductivity, (b) seebeck coefficient, (c) power factor.

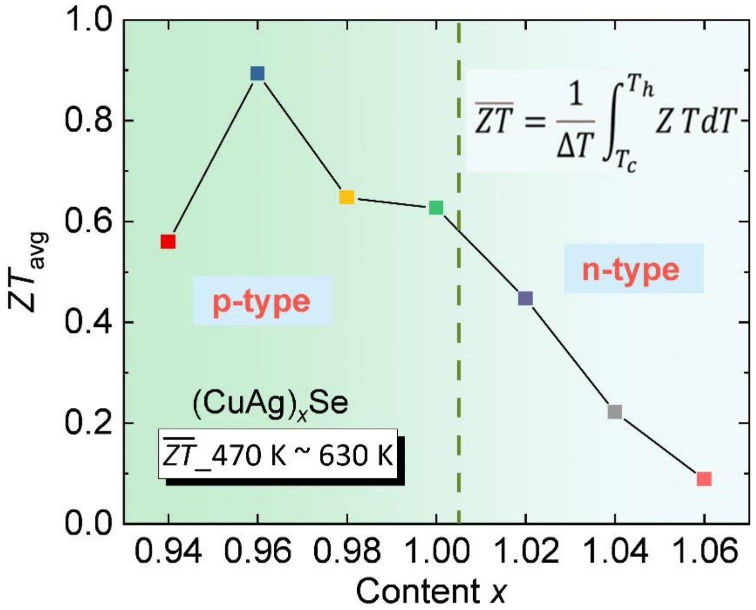

Fig. S8 The average *ZT* of $(CuAg)_x$Se (x = 0.94, 0.96, 0.98, 1, 1.02, 1.04, 1.06) of 470 ~ 630 K.

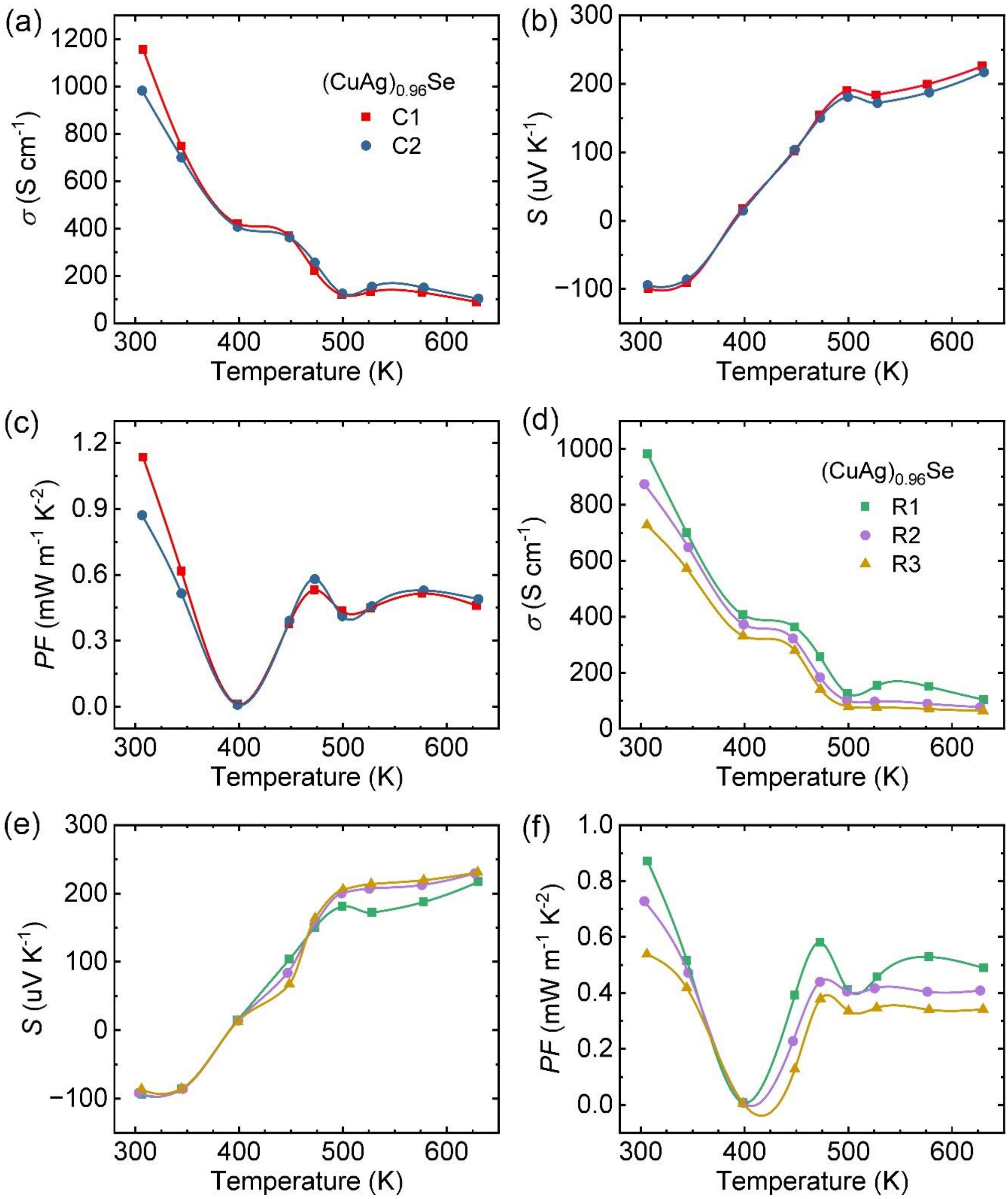

Fig. S9 The chemical composition reproducibility of temperature-dependent electric transport properties of $(CuAg)_{0.96}Se$ (C1 and C2 are sample-1 and sample-2 of different batches): (a) conductivity, (b) seebeck coefficient, (c) power factor; repeated cycle tests (R1, R2, R3) of sample-2: (d) conductivity, (e) seebeck coefficient, (f) power factor.

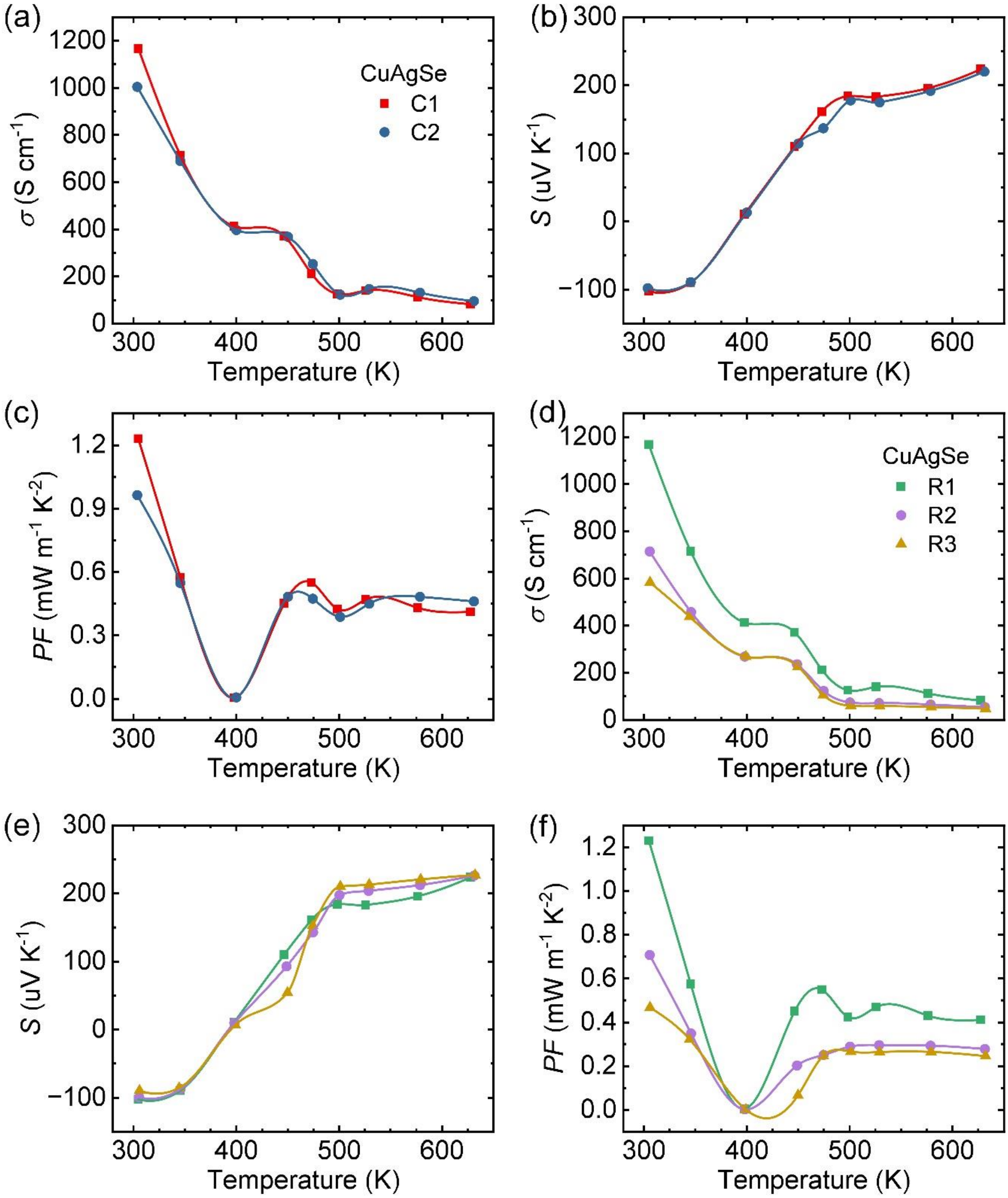

Fig. S10 The chemical composition reproducibility of temperature-dependent electric transport properties of CuAgSe (C1 and C2 are sample-1 and sample-2 of different batches): (a) conductivity, (b) seebeck coefficient, (c) power factor; repeated cycle tests (R1, R2, R3) of sample-1: (d) conductivity, (e) seebeck coefficient, (f) power factor.

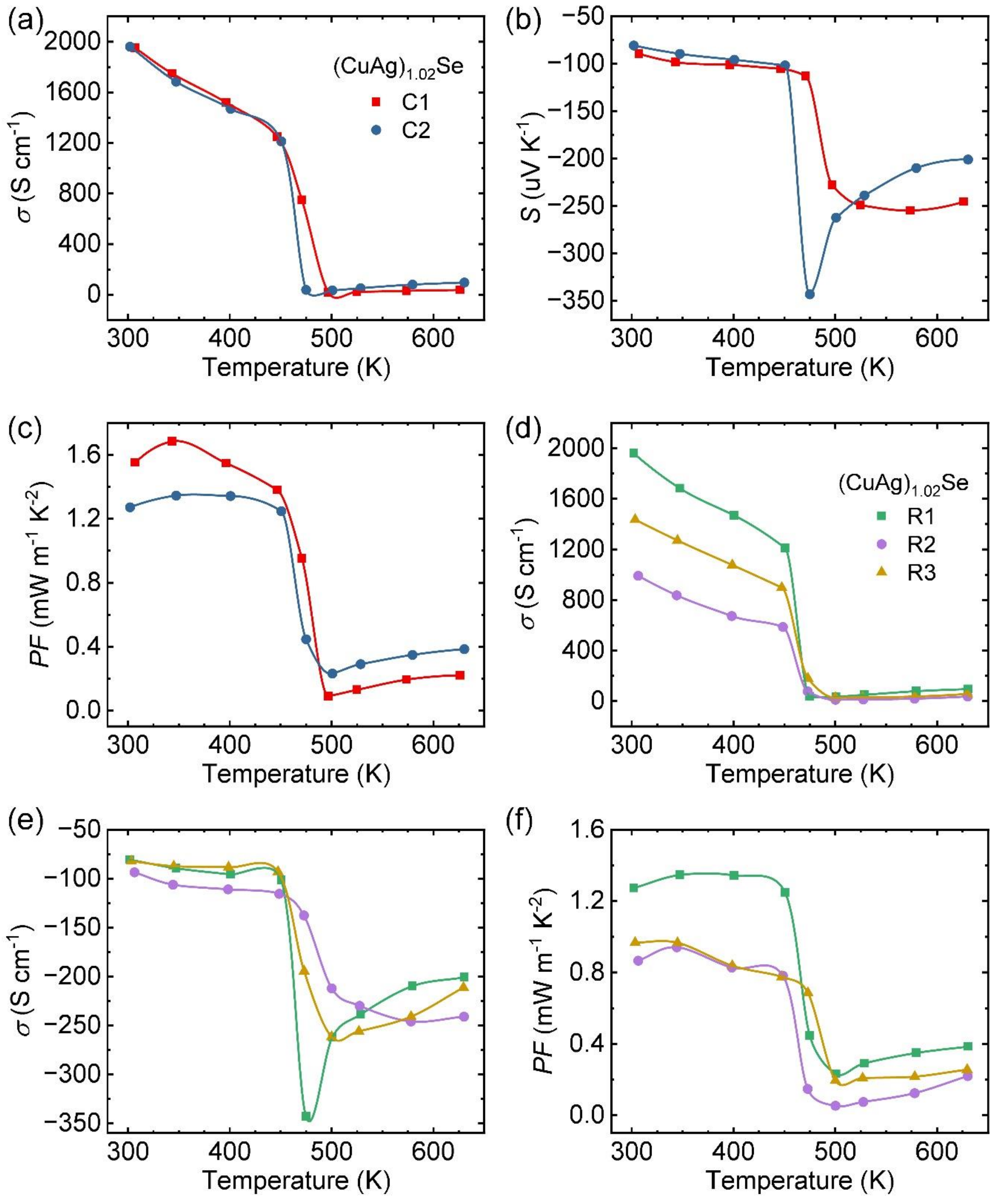

Fig. S11 The chemical composition reproducibility of temperature-dependent electric transport properties of $(CuAg)_{1.02}Se$ (C1 and C2 are sample-1 and sample-2 of different batches): (a) conductivity, (b) seebeck coefficient, (c) power factor; repeated cycle tests (R1, R2, R3) of sample-2: (d) conductivity, (e) seebeck coefficient, (f) power factor.

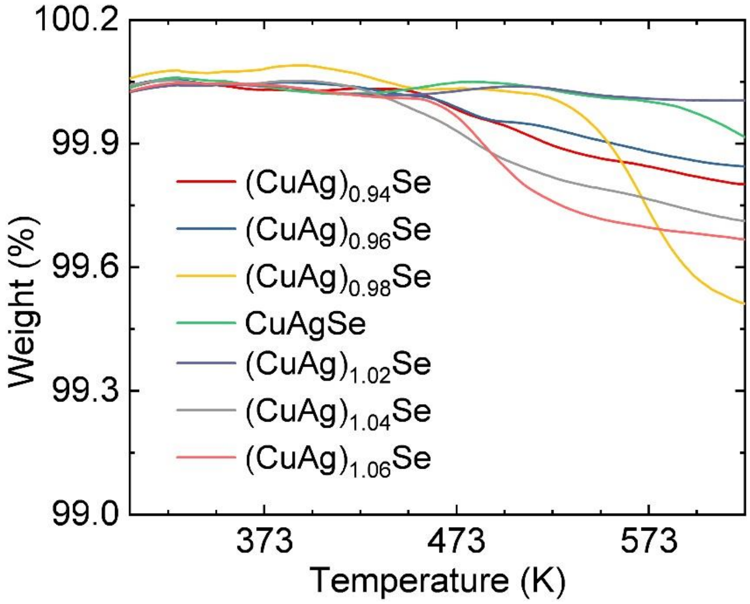

Fig. S12 Thermogravimetric curve of $(CuAg)_xSe$ from 300 K to 623 K (x = 0.94, 0.96, 0.98, 1, 1.02, 1.04, 1.06).

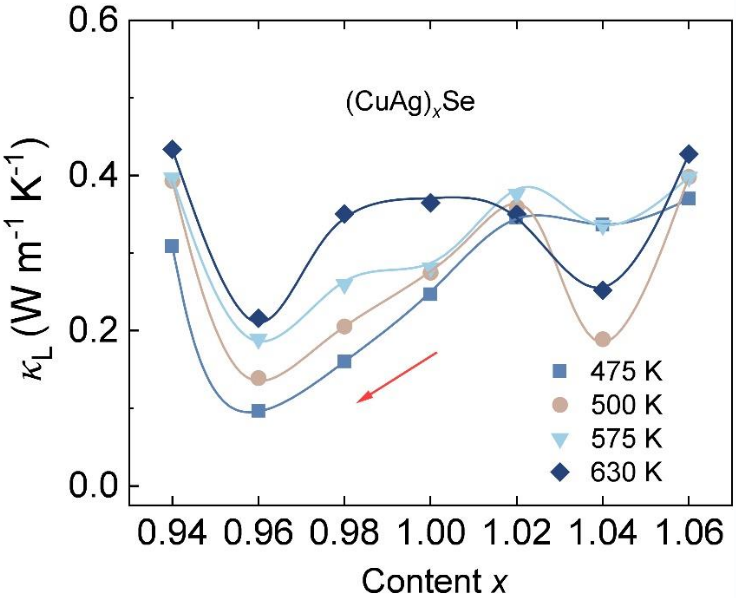

Fig. S13 The CuAg content x dependent lattice thermal conductivity at several different temperatures.

Supplementary Tables

Table S1. Positron lifetime τ_1 and τ_2, intensity of each lifetime component I_1 and I_2, average positron lifetime of $(CuAg)_xSe$ (x = 0.94, 0.96, 0.98, 1, 1.02, 1.04, 1.06).

samples	τ_1 (ps)	τ_2 (ps)	I_1 (%)	I_2(%)	Average lifetime (ps)
$(CuAg)_{0.94}Se$	143	272	13	87	255
$(CuAg)_{0.96}Se$	171	271	12	88	260
$(CuAg)_{0.98}Se$	176	272	17	83	262
CuAgSe	179	281	16	84	264
$(CuAg)_{1.02}Se$	148	289	15	85	267
$(CuAg)_{1.04}Se$	176	291	22	78	266
$(CuAg)_{1.06}Se$	159	290	16	84	269

Table S2. The Hall carrier concentration, Hall mobility, effective mass and relaxation time of $(CuAg)_xSe$ (x= 0.94, 0.96, 0.98, 1, 1.02, 1.04, 1.06) at room temperature.

samples	n_H (cm^{-3})	μ_H (cm^2 V^{-1} s^{-1})	m*/m$_e$	τ_R (10^{-13} s)
$(CuAg)_{0.94}Se$	-4.47×10^{18}	1714	0.135	1.315
$(CuAg)_{0.96}Se$	-4.02×10^{18}	1795	0.131	1.343
$(CuAg)_{0.98}Se$	-4.25×10^{18}	1763	0.142	1.431
CuAgSe	-3.35×10^{18}	2176	0.121	1.504
$(CuAg)_{1.02}Se$	-5.35×10^{18}	2286	0.125	1.627
$(CuAg)_{1.04}Se$	-3.88×10^{18}	2094	0.133	1.591
$(CuAg)_{1.06}Se$	-4.00×10^{18}	2582	0.111	1.636

Table S3. The temperature dependent Hall carrier concentration, hall mobility, effective mass of (a) $(CuAg)_{0.96}Se$, (b) CuAgSe and (c) $(CuAg)_{1.02}Se$.

(a)

$(CuAg)_{0.96}Se$	n_H (cm^{-3})	μ_H ($cm^2\ V^{-1}\ s^{-1}$)	m^*/m_e
323K	-4.46×10^{18}	1380	0.126
373K	-4.27×10^{18}	841	0.035
423K	-7.69×10^{18}	321	0.082
473K	-1.78×10^{19}	78	0.415
573K	-4.90×10^{20}	1.66	4.677
623K	-3.69×10^{20}	1.60	4.418

(b)

CuAgSe	n_H (cm^{-3})	μ_H ($cm^2\ V^{-1}\ s^{-1}$)	m^*/m_e
323K	-3.84×10^{18}	1569	0.116
373K	-3.71×10^{18}	936	0.035
423K	-6.47×10^{18}	378	0.077
473K	-1.46×10^{19}	91	0.385
573K	-4.78×10^{20}	1.49	4.458
623K	-3.28×10^{20}	1.61	4.024

(c)

$(CuAg)_{1.02}Se$	n_H (cm^{-3})	μ_H ($cm^2\ V^{-1}\ s^{-1}$)	m^*/m_e
323K	-4.31×10^{18}	2658	0.107
373K	-3.97×10^{18}	2491	0.097
423K	-5.28×10^{18}	1604	0.112
473K	-4.80×10^{18}	170	0.741
573K	-1.05×10^{18}	449	0.089
623K	-1.38×10^{18}	421	0.089

Table S4. The density values of $(CuAg)_xSe$ (x = 0.94, 0.96, 0.98, 1, 1.02, 1.04, 1.06).

Sample	Density (g/cm^3)
$(CuAg)_{0.94}Se$	6.89
$(CuAg)_{0.96}Se$	6.78
$(CuAg)_{0.98}Se$	6.84
CuAgSe	7.19
$(CuAg)_{1.02}Se$	7.17
$(CuAg)_{1.04}Se$	6.94
$(CuAg)_{1.06}Se$	7.15

Table S5. The Lorentz number (a) calculated according to equation (13), (b) obtained by equation: $L = 1.5 + \exp\left[-\frac{|S|}{116}\right]$.

(a)

L ($V^2 K^{-2}$)	$(CuAg)_{0.96}Se$	$(CuAg)_{0.98}Se$	CuAgSe	$(CuAg)_{1.02}Se$	$(CuAg)_{1.04}Se$
303 K	1.92×10^{-8}	1.90×10^{-8}	1.90×10^{-8}	2.02×10^{-8}	1.90×10^{-8}
348 K	1.96×10^{-8}	1.97×10^{-8}	1.97×10^{-8}	1.97×10^{-8}	1.86×10^{-8}
400 K	2.41×10^{-8}	2.41×10^{-8}	2.43×10^{-8}	1.93×10^{-8}	1.84×10^{-8}
450 K	1.91×10^{-8}	1.92×10^{-8}	1.87×10^{-8}	1.91×10^{-8}	1.81×10^{-8}
475 K	1.71×10^{-8}	1.68×10^{-8}	1.70×10^{-8}	1.51×10^{-8}	1.62×10^{-8}
500 K	1.64×10^{-8}	1.64×10^{-8}	1.65×10^{-8}	1.55×10^{-8}	1.88×10^{-8}
523 K	1.65×10^{-8}	1.63×10^{-8}	1.65×10^{-8}	1.57×10^{-8}	2.44×10^{-8}
573 K	1.62×10^{-8}	1.62×10^{-8}	1.63×10^{-8}	1.61×10^{-8}	1.54×10^{-8}
630 K	1.58×10^{-8}	1.58×10^{-8}	1.59×10^{-8}	1.62×10^{-8}	1.58×10^{-8}

(b)

L ($V^2 K^{-2}$)	$(CuAg)_{0.96}Se$	$(CuAg)_{0.98}Se$	CuAgSe	$(CuAg)_{1.02}Se$	$(CuAg)_{1.04}Se$
303 K	1.93×10^{-8}	1.91×10^{-8}	1.91×10^{-8}	2.00×10^{-8}	1.91×10^{-8}
348 K	1.96×10^{-8}	1.97×10^{-8}	1.96×10^{-8}	1.96×10^{-8}	1.88×10^{-8}
400 K	2.36×10^{-8}	2.35×10^{-8}	2.41×10^{-8}	1.94×10^{-8}	1.86×10^{-8}
450 K	1.92×10^{-8}	1.92×10^{-8}	1.89×10^{-8}	1.92×10^{-8}	1.84×10^{-8}
475 K	1.76×10^{-8}	1.74×10^{-8}	1.75×10^{-8}	1.55×10^{-8}	1.68×10^{-8}
500 K	1.69×10^{-8}	1.70×10^{-8}	1.71×10^{-8}	1.60×10^{-8}	1.90×10^{-8}
523 K	1.70×10^{-8}	1.69×10^{-8}	1.71×10^{-8}	1.63×10^{-8}	2.45×10^{-8}
573 K	1.68×10^{-8}	1.68×10^{-8}	1.69×10^{-8}	1.66×10^{-8}	1.59×10^{-8}
630 K	1.64×10^{-8}	1.64×10^{-8}	1.65×10^{-8}	1.68×10^{-8}	1.64×10^{-8}

Table S6. The grain size of $(CuAg)_xSe$ (x = 0.94, 0.96, 0.98, 1, 1.02, 1.04, 1.06) obtained from XRD diffraction peaks.

Sample	Grain size (nm)
$(CuAg)_{0.94}Se$	30
$(CuAg)_{0.96}Se$	26
$(CuAg)_{0.98}Se$	36
CuAgSe	33
$(CuAg)_{1.02}Se$	35
$(CuAg)_{1.04}Se$	25
$(CuAg)_{1.06}Se$	29